

Critical currents and pinning forces in $\text{Nd}_{2-x}\text{Ce}_x\text{CuO}_{4-\delta}$ thin films

Carla Cirillo, Anita Guarino, Angela Nigro, and Carmine Attanasio*

*Laboratorio Regionale SuperMat, CNR-INFM Salerno and Dipartimento di Fisica "E. R. Caianiello",
Università degli Studi di Salerno, Baronissi, Salerno I-84081, Italy*

(Received 27 November 2008; revised manuscript received 31 March 2009; published 23 April 2009)

Critical current density, J_c , and flux-pinning force density, F_p , have been investigated at different temperatures in electron-doped $\text{Nd}_{2-x}\text{Ce}_x\text{CuO}_{4-\delta}$ thin films for magnetic fields, H , applied parallel to the c axis. The reduced pinning force density $f \equiv F_p/F_p^{\text{max}}$ shows a clear scaling behavior when H is normalized to the irreversibility field H^* , indicating the presence of the same pinning mechanism in the investigated temperature range. Moreover the maximum of F_p as function of the field at each temperature depends linearly on H^* . The experimental data, interpreted using a modified Anderson-Kim description of the flux-creep theory, imply a magnetic field dependence of the activation energy $U(H) \sim H^{-\alpha}$ with $\alpha=0.8$. This value indicates that in $\text{Nd}_{2-x}\text{Ce}_x\text{CuO}_{4-\delta}$ a quasi-two-dimensional vortex system is present, intermediate between Bi-based and Y-based hole-doped compounds.

DOI: 10.1103/PhysRevB.79.144524

PACS number(s): 74.25.Qt, 74.25.Sv, 74.72.Jt

I. INTRODUCTION

The scaling law of the flux-pinning force density F_p ($F_p = J_c B = \mu_0 J_c H$) is a well-known argument in conventional superconductors¹⁻³ and is typically described in the framework of the flux-line shear (FLS) model.³ In this model, where the flux lines are supposed to move along weak-pinning percolative paths, the theoretical description predicts a quadratic dependence of F_p at high magnetic fields, i.e., $F_p \sim (H/H_{c2})^{1/2}(1-H/H_{c2})^2$, where H_{c2} is the upper critical magnetic field.^{3,4}

In the case of high- T_c superconductors (HTS) F_p evaluated from J_c transport measurements have shown a scaling behavior if a reduced magnetic field $h \equiv H/H^*$ is introduced. H^* is the irreversibility field and in type-II superconductors it is usually defined via magnetic measurements: it is the field above which the magnetization becomes reversible (and hence J_c becomes zero).⁵ The study of the irreversibility field in HTS has been a very active field of research because H^* is a measure of the pinning strength and its knowledge can give information about the mechanisms determining the critical current density J_c .^{6,7} The scaling of F_p versus h has been observed in several specimens on different hole-doped HTS cuprates such as $\text{YBa}_2\text{Cu}_3\text{O}_x$ (Refs. 6 and 8) and $\text{Bi}_2\text{Sr}_2\text{Ca}_2\text{Cu}_3\text{O}_x$ high-quality epitaxial films,⁷ $\text{Bi}_2\text{Sr}_2\text{Ca}_1\text{Cu}_2\text{O}_x$ melt-processed samples,⁹ or thin films.¹⁰ While a large number of papers have been dedicated to the study of the transport and magnetic properties in electron-doped copper oxide superconductors such as, for example, $\text{Nd}_{2-x}\text{Ce}_x\text{CuO}_{4-\delta}$ (NCCO),¹¹⁻¹⁶ nothing has been specifically reported about the presence of possible scaling laws of the pinning force in these systems. This kind of investigation is however very important in defining the possibility of applications of these materials.

$\text{Nd}_{2-x}\text{Ce}_x\text{CuO}_{4-\delta}$ crystallizes in the so-called T' structure, which is characterized by the absence of the apical oxygen. Superconductivity occurs in a narrow range of Ce doping: $0.10 < x < 0.24$ with the highest $T_c \approx 24$ K at a doping level of about 0.15.¹⁷ Unlike hole-doped materials, the electron-doped compounds require a careful oxygen-reduction an-

nealing to achieve superconductivity. The physical properties of the n -type family have been measured mainly on bulk and single crystals, and compared with the hole-doped properties, a number of differences related to the electronic phase diagram and to the symmetry of the superconducting order parameter for the two HTS family have been reported.^{18,19} On the other hand investigation on thin films are limited by the difficulties in the sample preparation arising from the critical values of both the charge carriers and the oxygen vacancies required to induce superconductivity. In the group of the HTS, only the electron-doped cuprates can be doped with two types of charge carriers at the same time, by means of cerium and oxygen. This unusual scenario supports theoretical models in which both electrons and holes can participate to the superconducting phenomenon, and same experimental results point out the existence of the two contributions together.²⁰ Then the study also of the overdoped regime becomes interesting because, within an appropriate window of cerium doping, one can study, for example, how the Hall coefficient changes sign as a function of temperature which is consistent with this two carrier scenario.²¹⁻²³

In this paper we report on electrical transport properties in overdoped $\text{Nd}_{2-x}\text{Ce}_x\text{CuO}_{4-\delta}$ thin films with $x=0.17$. Critical current densities have been measured for different values of the temperature as function of the external magnetic field. We have observed a scaling behavior of the normalized pinning force density $f \equiv F_p/F_p^{\text{max}}$ (here F_p^{max} is the maximum of the pinning force density at each temperature) versus the reduced field h . The experimental data have been interpreted in the entire magnetic-field range in the framework of a model¹⁰ based on the classical Anderson-Kim (AK) theory of the flux creep.²⁴

II. SAMPLE PREPARATION AND ELECTRICAL CHARACTERIZATION

$\text{Nd}_{1.83}\text{Ce}_{0.17}\text{CuO}_{4-\delta}$ c -axis oriented thin films have been prepared using a deposition technique based on a planar dc diode sputtering configuration, where the substrate was positioned on a heater in front of the sputtering source. A single

stoichiometric target, homemade by an optimized sintered fabrication method, has been used as a sputtering source.²⁵ The films were deposited on (001) SrTiO₃ substrates heated at $T=850$ °C in mixed atmosphere of argon and oxygen at a total pressure of 1.7 mbar in the deposition chamber. After the deposition, the films were annealed during 30 min in vacuum at the same deposition temperature. A second annealing step, for 60 min at $T=900$ °C, in ambient argon atmosphere was performed in order to further reduce the oxygen content in the films. The deposition rate was 1.2 nm/min while the typical film thickness was around 200 nm. More detailed information about the fabrication procedure will be reported in a forthcoming paper. The cerium content ($x=0.17$) was evaluated by wavelength dispersive spectroscopy (WDS). Transport properties were performed using a standard dc four-probe technique.

The superconducting transition temperature values T_c , defined as the midpoint of the resistive transition curve, were around 9 K. The resistivity values measured in the normal state at $T=30$ K were $\rho(30\text{ K}) \approx 60\ \mu\Omega\text{ cm}$. These values are a bit different from what was reported in the literature probably due to the nonoptimal oxygen content in our Ce overdoped samples.²⁶ The residual resistivity ratio, $\beta \equiv \rho(300\text{ K})/\rho(30\text{ K})$, was typically around three. Current-voltage (I - V) characteristics were measured on an unstructured sample 2 mm wide. The length between the voltage contacts was 3 mm. Magnetic fields were always applied perpendicular to the surface of the substrate, i.e., parallel to the c axis of the film. The critical current densities J_c at $T=2.1$ K and in zero field can be roughly estimated to be of the order of $3 \times 10^8\text{ A/m}^2$, and they were defined by the electric field criterion $E=E_c=4 \times 10^{-5}\text{ V/cm}$. The values of the measured critical current density are slightly lower with respect to some others reported in the literature which refer to epitaxial thin films.²⁷

III. RESULTS AND DISCUSSION

In Fig. 1 I - V curves at $T=4.2$ K in various applied magnetic fields are shown. We see that for $\mu_0 H=3000$ Oe an Ohmic behavior is observed over the entire range. According to the literature we can define this as the irreversibility field H^* at this temperature.^{28,29}

In Fig. 2 the dependence of the critical current density J_c on the external magnetic field for five different temperatures is shown. Apart from the aforementioned slightly low values of J_c , its general features are very similar to what was measured in hole-doped HTS with a stronger depression at higher temperatures and lower magnetic fields.⁷

In Fig. 3 the flux-pinning force density, as calculated from data of Fig. 2, versus the magnetic field is shown. When the magnetic field is normalized as $h \equiv H/H^*$ and the pinning force density as $f \equiv F/F_p^{\max}$, a clear scaling behavior is observed (see Fig. 4). In Fig. 4 the dashed line is the curve obtained using the expression $f(h) \sim h^{1/2}(1-h)^2$ valid in the FLS model. As we can see this model cannot satisfactorily explain the general features of the temperature scaling of the $f(h)$ curve including the curvature at intermediate reduced fields (between 0.3 and 0.8) and the tail at high magnetic

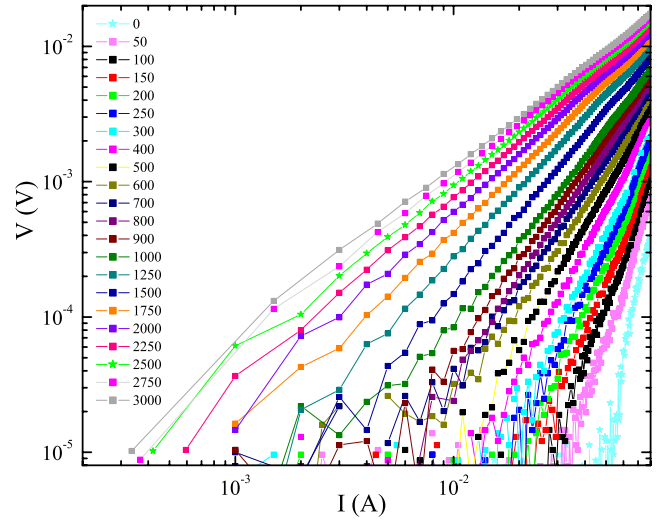


FIG. 1. (Color online) I - V characteristics in double-logarithmic scale at $T=4.2$ K at various magnetic fields. Numbers in the figure indicate the values of the fields in Oe.

fields. The comment to the solid line in the figure, which is central in the paper, will be given later.

Figure 5 shows the Arrhenius plots of the resistive transitions at different applied magnetic fields for the sample whose critical current-density data are shown in the previous figures. The curves have been taken using for the bias density current the value $J=1.2 \times 10^5\text{ A/m}^2$. The plots are linear in a wide $1/T$ interval indicating that the resistance is due to a thermally activated process in this temperature range. In the limit of low current density and linear regime, the resistance can be written in the form $R(T,H)=R_0 \exp[-U_0(T,H)/k_B T]$, where $U_0(T,H)$ is the activation energy for $J \approx 0$, and then the slopes of the curves plotted in Fig. 5 give directly the values of the activation energy at different H values.^{7,29,30} The inset of Fig. 5, where the activation energy is plotted as a function of H in a log-log scale, indicates that U_0 is proportional to $H^{-\alpha}$ with $\alpha=0.8$.

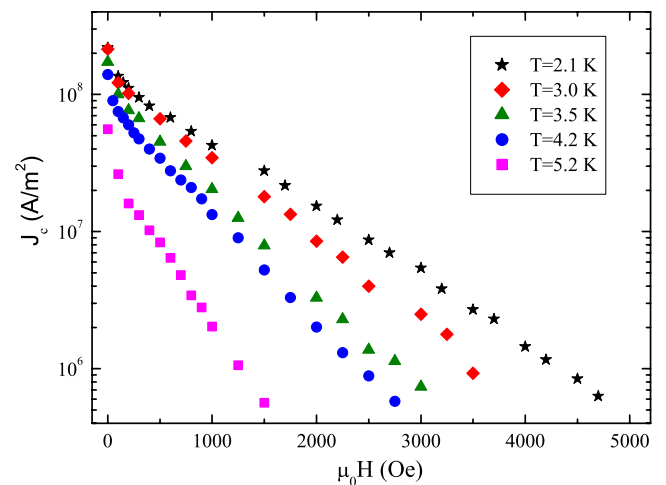


FIG. 2. (Color online) Critical current density as function of the magnetic field for five different temperatures. From left to right: $T=5.2$ K, $T=4.2$ K, $T=3.5$ K, $T=3.0$ K, and $T=2.1$ K.

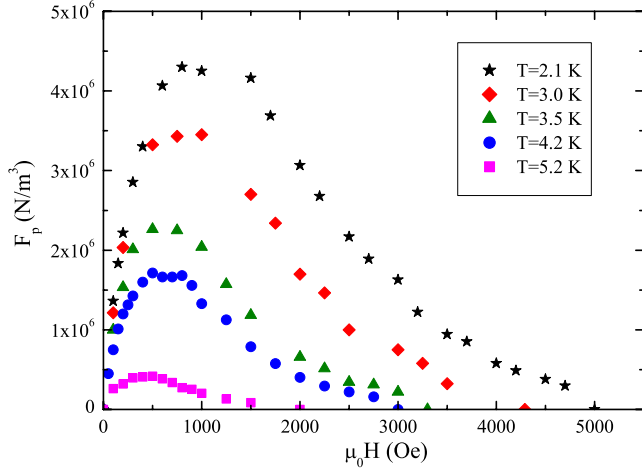


FIG. 3. (Color online) Pinning force density as function of the magnetic field for five different temperatures. From bottom to up: $T=5.2$ K, $T=4.2$ K, $T=3.5$ K, $T=3.0$ K, and $T=2.1$ K.

To account for the pinning force scaling behavior shown in Fig. 4, we start from the AK model²⁴ in which the I - V curves are expressed as

$$E = Ba_0\nu_0 \exp\left(-\frac{U_{\text{eff}}(T,H,J)}{k_B T}\right), \quad (1)$$

where E is the electric field due to the motion of the flux bundles, B is the magnetic-field induction, ν_0 is an attempt frequency of the vortices which try to escape the potential well, and a_0 is the intervortex distance. U_{eff} is the effective activation energy. Assuming the multiplicative character of the activation energy we can write $U_{\text{eff}}=U_0(T,H)\eta(J/J_{c0})$,^{7,10} where $U_0(T,H)$, as defined above, is the height of the potential barrier at $J=0$. J_{c0} is the critical current density when there is no thermal activation and is determined as $J_{c0}=cU_0/(BV_a X_p)$, where c is a con-

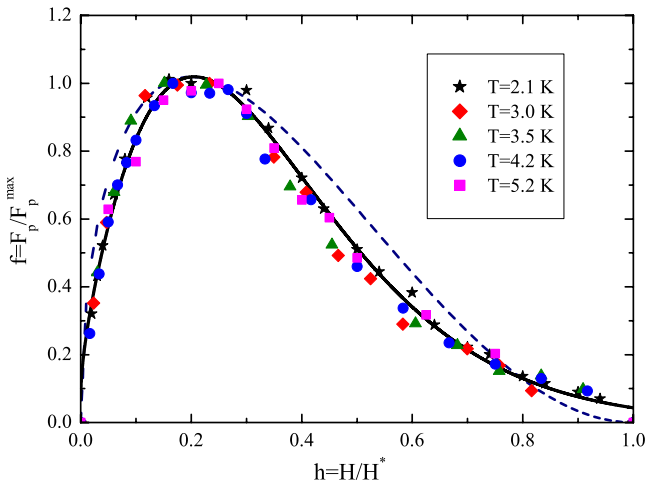


FIG. 4. (Color online) Temperature scaling of the normalized pinning force density versus the reduced field. Symbols are defined in the figure. The dashed line is the curve obtained using the FLS model. The solid line is the fit to experimental data using the model described in the text.

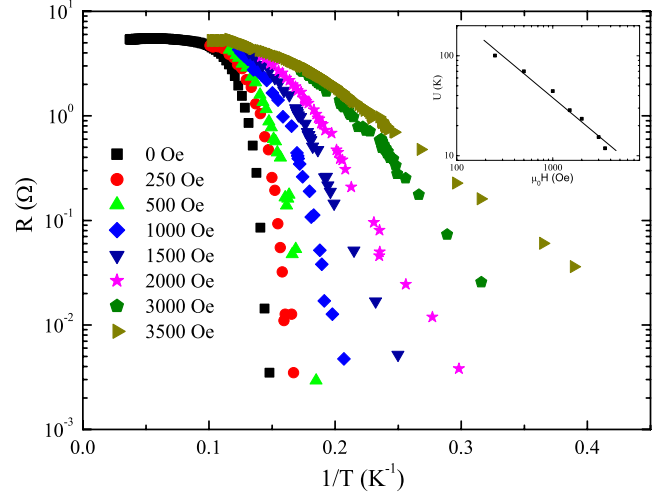


FIG. 5. (Color online) Arrhenius plots of the resistance $R(T,H)$ for different values of the magnetic fields, indicated by the numbers in the figure. Inset: Magnetic-field dependence of the activation energy U_0 . The solid line is the fit to the data with $U_0 \propto H^{-0.8}$.

stant, V_a is the correlation volume of a flux bundle, and X_p is the effective range of the potential energy, that is, the average distance among the pinning centers. The height of the potential barrier at $J=0$ is usually written as $U_0(T,H)=a(T)H^{-\alpha}$, where $a(T)$ is a generic function of the temperature which goes to zero when T approaches T_c .³¹ Such behavior for $U_0(T,H)$ has been predicted and observed by transport measurements on Y-based copper oxide compounds with $\alpha=1$ (Refs. 31–33) and on Bi-based compounds above the irreversibility line with $\alpha=0.5$.^{7,10,30,34–36}

Following the model already applied in describing experimental data on high-quality $\text{Bi}_2\text{Sr}_2\text{Ca}_1\text{Cu}_2\text{O}_x$ thin films deposited by molecular-beam epitaxy (MBE),¹⁰ the critical electric field E_c can be obtained from Eq. (1) by setting $J=J_c$. So we get

$$E_c = Ba_0\nu_0 \exp\left\{-\frac{\beta^*}{\eta(0)}\left(\frac{H^*(T)}{H}\right)^\alpha \eta\left[J_c\left(\frac{H^*(T)}{H}\right)^\alpha \frac{\eta(0)}{\beta^* C}\right]\right\}, \quad (2)$$

where $\beta^* \equiv \ln(B^* a_0 \nu_0 / E_c)$ and $C = c / (BV_a X_p)$. The final expression for the pinning force is then

$$F_p = J_c B = \mu_0 J_c H = \mu_0 C \beta^* H^*(T) \times \left[\frac{H}{H^*(T)}\right]^{1-\alpha} [\eta(0)]^{-1} \eta^{-1} \left[\eta(0) \frac{\beta}{\beta^*} \left(\frac{H}{H^*(T)}\right)^\alpha\right]. \quad (3)$$

The explicit expression of the function $\eta(J)$ is determined by the actual dependence of the pinning potential on the spatial coordinates $U(x)$.³⁷ Assuming a sinusoidal dependence for $U(x)$ and introducing a distribution for the critical current densities^{10,38} one can justify the logarithmic form for $\eta(J) = -\bar{\eta} \ln(J/\delta J_{c0})$,^{10,39} where $\delta=8/9$ and $\bar{\eta}=6/(6 \ln \zeta_c + 5)$. $\zeta_c = x_c/x_0$, where x_0 represents the central point of the potential well and x_c is a cutoff distance beyond which $U(x)$ is zero. Putting this expression for $\eta(J)$ in Eq. (3) it is easy to see that the maximum of the pinning force F_p^{max} depends linearly

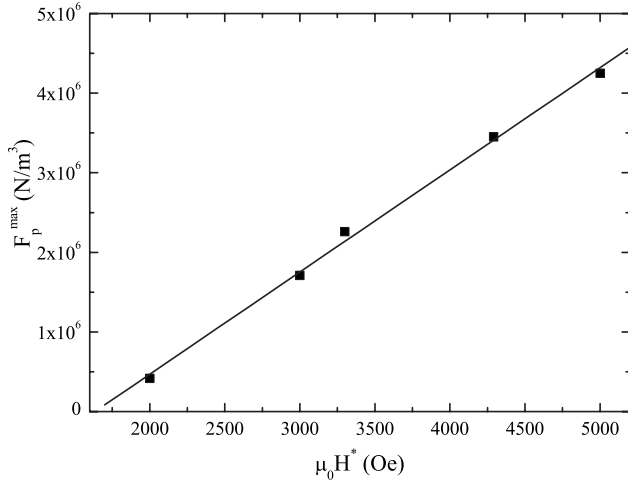


FIG. 6. Dependence of F_p^{\max} on H^* . The solid line is a guide to the eye.

on the irreversibility field and one can explain the experimental data shown in Fig. 6. This result shows that the above description for the pinning force does contain this feature and it is not in contradiction to what was also obtained in other models such as, for example, FLS or collective pinning.⁴⁰

Using the expression given above for $\eta(J)$, Eq. (3) can be also normalized by F_p^{\max} obtaining

$$f(h) \sim h^{1-\alpha} \exp\{-(h^\alpha/\bar{\eta})(1 + \ln h/\beta^*)\}. \quad (4)$$

The thick solid line in Fig. 4 is the best fit to the experimental data from which we obtain $\bar{\eta}=0.44 \pm 0.05$ and $\beta^*=0.55 \pm 0.01$. The parameter α has been kept fixed during the fitting procedure to the value of 0.8 as independently obtained from the resistive transitions. The above analysis, based on the flux-creep theory, shows that, also in electron-doped $\text{Nd}_{2-x}\text{Ce}_x\text{CuO}_{4-\delta}$ HTS, F_p scales with H/H^* instead of H/H_{c2} . From the obtained value of the parameter $\bar{\eta}$ we get that $\zeta_c=8.2$ which is almost one order of magnitude higher than the range of the pinning potential found for $\text{Bi}_2\text{Sr}_2\text{Ca}_1\text{Cu}_2\text{O}_x$ thin films¹⁰ but smaller than the one evaluated in $\text{YBa}_2\text{Cu}_3\text{O}_{7-\delta}$ thin films.³⁹ As largely discussed in the literature^{7,30,41,42} the value of the exponent α in the activation energy dependence reflects the different topology of the vortices in a superconductor, and it is related also to the disorder and to the magnetic field. In highly anisotropic Bi-based systems the vortex lattice deforms, plastically forming double kinks in the superconducting planes [two-dimensional (2D) pancake vortices] which implies $U_{\text{eff}} \sim H^{-0.5}$.⁴² On the contrary, in less anisotropic Y-based samples the densely entangled vortex lattice shears without any kink in the superconducting planes [three-dimensional (3D) anisotropic vortices] and this explains the observed $U_{\text{eff}} \sim H^{-1}$ relation in these systems.^{29,43} Here we want to say that a satisfactory fit of the reduced pinning force data can also be obtained using a modified FLS model when taking into account the existence of distribution of the superconducting properties in the sample.⁴⁰ However, even if this possibility cannot be definitely ruled out, we believe that the proved existence of a

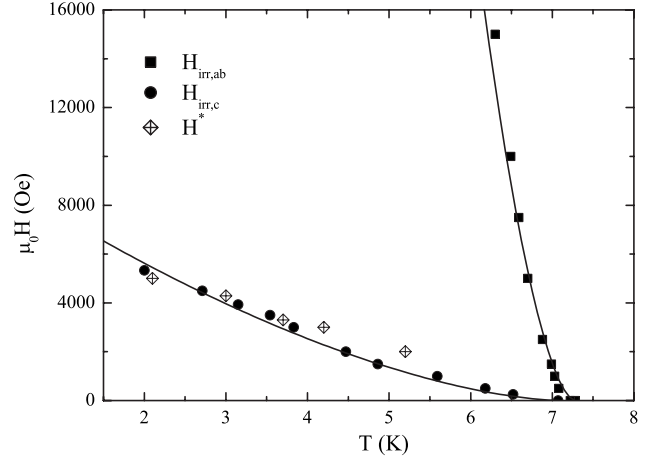


FIG. 7. Temperature dependence of the parallel (closed squares) and perpendicular (closed circles) irreversibility fields for the $\text{Nd}_{1.83}\text{Ce}_{0.17}\text{CuO}_{4-\delta}$ film as derived from the resistive transition measurements. Diamonds represent the field H^* as derived from I - V measurements. The solid lines are fits to the equation $H_{\text{irr}} = H_{\text{irr}}(0)(1 - T/T_{c0})^\mu$, see text.

thermally activated mechanism in the transport properties of our system gives a strong support to the correctness of using a modified AK model to explain the experimental data.

The quasi-2D character of the vortex system in $\text{Nd}_{1.83}\text{Ce}_{0.17}\text{CuO}_{4-\delta}$ can also be tested by roughly estimating the value of the vortex correlation length along the c direction, L_c .⁴⁴ In fact, in the case of a 3D system the vortex correlation length should be limited by the film thickness while in the 2D case L_c should be shorter than the sample vertical dimension. The current density J^+ at the onset of the nonlinear behavior can be used to extract an upper limit for L_c through the relation $J^+\Phi_0 L_c R_{ab} \approx k_B T$,^{44,45} where Φ_0 is the magnetic-flux quantum and R_{ab} is the correlation length perpendicular to the c axis. From Fig. 1, at $T=4.2$ K and $\mu_0 H=2750$ Oe, we obtain $J^+ \approx 1.66 \times 10^8$ A/m² and then $L_c R_{ab}=250$ nm². Assuming $R_{ab} \approx 2a_0 = 2\sqrt{\Phi_0/\mu_0 H}$ we obtain $R_{ab}=180$ nm and consequently $L_c=1.4$ nm which is much smaller than the film thickness. Following the same reasoning at the higher temperature ($T=5.2$ K for $\mu_0 H=1750$ Oe), we get $J^+ \approx 2.0 \times 10^6$ A/m² and then $L_c=113$ nm which is still half of the sample thickness.

The weaker two-dimensional character of the $\text{Nd}_{1.83}\text{Ce}_{0.17}\text{CuO}_{4-\delta}$ system is finally confirmed if the anisotropy coefficient at zero temperature, $\gamma(0) = H_{\text{irr},ab}(0)/H_{\text{irr},c}(0)$, is derived from the temperature dependence of the irreversibility field perpendicular, $H_{\text{irr},ab}(T)$, and parallel to the c axis, $H_{\text{irr},c}(T)$. The irreversibility fields in both directions have been determined taking the 10% of the superconducting transition curves at fixed temperature as function of the applied field (or, occasionally, at fixed field as function of the temperature). Of course, the absolute position of the irreversibility lines in both directions in the H - T plane depends on the adopted criterion but very similar results have been obtained when defining, for example, H_{irr} as the field where $R=0.01R_N$, R_N being the resistance of the sample just before the superconducting transition. In Fig. 7 the irreversibility fields H_{irr} in both directions are reported together

with the irreversibility fields H^* as determined from the I - V measurements. With the adopted criterion the H^* and $H_{\text{irr},c}$ points lie very close to each other in the phase diagram. The irreversibility lines in both directions display a positive curvature^{46–49} and they can both be fitted to an equation of the form $H_{\text{irr}}=H_{\text{irr}}(0)(1-T/T_{c0})^\mu$,^{29,50,51} where T_{c0} is the zero-field transition temperature, and $H_{\text{irr}}(0)$ and μ are fitting parameters. The fits, shown as solid lines in Fig. 7, gave as a result: $H_{\text{irr},c}(0)=9550\pm 800$ Oe and $\mu_c=1.60\pm 0.05$ for $H\parallel c$, and $H_{\text{irr},ab}(0)=390\,000\pm 15\,000$ Oe and $\mu_{ab}=1.70\pm 0.05$ for $H\parallel ab$. The ratio between $H_{\text{irr},ab}(0)$ and $H_{\text{irr},c}(0)$ gives as a value of the anisotropy coefficient $\gamma=41\pm 5$. This value, similar to what was measured in $\text{Nd}_{1.85}\text{Ce}_{0.15}\text{CuO}_{4-\delta}$ single crystals,^{14,46} is more than one order of magnitude smaller than the anisotropy factors reported for Bi-based compounds⁵² but it is six times larger than the typical γ values reported for Y-based compounds.^{29,50,53}

IV. CONCLUSIONS

In conclusion, we have measured electric transport properties on overdoped $\text{Nd}_{2-x}\text{Ce}_x\text{CuO}_{4-\delta}$ ($x=0.17$) thin films for different values of the temperature and external magnetic fields. The observed scaling behavior of the reduced pinning force f versus the normalized magnetic field h has been interpreted in the framework of the AK model of the flux creep. The obtained exponent $\alpha=0.8$ for the magnetic-field dependence of the activation energy, $U(H)\sim H^{-\alpha}$, is related to the (anisotropic) three-dimensional nature of the vortex lattice due to the relatively large anisotropy of the system. Our transport measurements show that, concerning the vortex lattice anisotropy, overdoped $\text{Nd}_{2-x}\text{Ce}_x\text{CuO}_{4-\delta}$ is somehow an intermediate system between Bi-based and Y-based compounds.

*Corresponding author; FAX: +39-089-965275; attanasio@sa.infn.it

¹W. A. Fietz and W. W. Webb, Phys. Rev. **178**, 657 (1969).

²A. M. Campbell and J. E. Evetts, Adv. Phys. **21**, 199 (1972).

³E. J. Kramer, J. Appl. Phys. **44**, 1360 (1973).

⁴L. Le Lay, T. C. Willis, and D. C. Larbalestier, Appl. Phys. Lett. **60**, 775 (1992).

⁵K. A. Müller, M. Takashige, and J. G. Bednorz, Phys. Rev. Lett. **58**, 1143 (1987).

⁶J. D. Hettinger, A. G. Swanson, W. J. Skocpol, J. S. Brooks, J. M. Graybeal, P. M. Mankiewich, R. E. Howard, B. L. Straughn, and E. G. Burkhardt, Phys. Rev. Lett. **62**, 2044 (1989).

⁷H. Yamasaki, K. Endo, S. Kosaka, M. Umeda, S. Yoshida, and K. Kajimura, Phys. Rev. Lett. **70**, 3331 (1993).

⁸R. Würdenweber and M. O. Abd-El-Hamed, J. Appl. Phys. **71**, 808 (1992).

⁹T. Matsushita, A. Matsuda, and K. Yanagi, Physica C **213**, 477 (1993).

¹⁰S. L. Prischepa, C. Attanasio, C. Coccorese, L. Maritato, F. Pourtier, M. Salvato, and V. N. Kushnir, J. Appl. Phys. **79**, 4228 (1996).

¹¹Y. Tokura, H. Takagi, and S. Uchida, Nature (London) **337**, 345 (1989).

¹²Minoru Suzuki and Makoto Hikita, Phys. Rev. B **41**, 9566 (1990).

¹³N.-C. Yeh, U. Kriplani, W. Jiang, D. S. Reed, D. M. Strayer, J. B. Barner, B. D. Hunt, M. C. Foote, R. P. Vasquez, A. Gupta, and A. Kussmaul, Phys. Rev. B **48**, 9861 (1993).

¹⁴H. Iwasaki, T. Matsumoto, F. Yukimachi, K. Tanigawa, and F. Matsuoka, Physica C **305**, 11 (1998).

¹⁵M. C. de Andrade, N. R. Dilley, F. Ruess, and M. B. Maple, Phys. Rev. B **57**, R708 (1998).

¹⁶Yayu Wang, S. Ono, Y. Onose, G. Gu, Yoichi Ando, Y. Tokura, S. Uchida, and N. P. Ong, Science **299**, 86 (2003).

¹⁷Y. Krockenberger, J. Kurian, A. Winkler, A. Tsukada, M. Naito, and L. Alff, Phys. Rev. B **77**, 060505(R) (2008).

¹⁸Dong Ho Wu, Jian Mao, S. N. Mao, J. L. Peng, X. X. Xi, T. Venkatesan, R. L. Greene, and Steven M. Anlage, Phys. Rev.

Let. **70**, 85 (1993).

¹⁹G. Blumberg, A. Koitzsch, A. Gozar, B. S. Dennis, C. A. Kendziora, P. Fournier, and R. L. Greene, Phys. Rev. Lett. **88**, 107002 (2002).

²⁰M. Imada, Rev. Mod. Phys. **70**, 1039 (1998).

²¹P. Fournier, X. Jiang, W. Jiang, S. N. Mao, T. Venkatesan, C. J. Lobb, and R. L. Greene, Phys. Rev. B **56**, 14149 (1997).

²²J. S. Higgins, Y. Dagan, M. C. Barr, B. D. Weaver, and R. L. Greene, Phys. Rev. B **73**, 104510 (2006).

²³J. Gauthier, S. Gagné, J. Renaud, M.-È. Gosselin, P. Fournier, and P. Richard, Phys. Rev. B **75**, 024424 (2007).

²⁴P. W. Anderson and Y. B. Kim, Rev. Mod. Phys. **36**, 39 (1964).

²⁵S. Uthayakumar, R. Fittipaldi, A. Guarino, A. Vecchione, A. Romano, A. Nigro, H.-U. Habermeier, and S. Pace, Physica C **468**, 2271 (2008).

²⁶F. Gollnik and M. Naito, Phys. Rev. B **58**, 11734 (1998).

²⁷H. Haensel, A. Beck, F. Gollnik, R. Gross, R. P. Huebener, and K. Knorr, Physica C **244**, 389 (1995).

²⁸W. K. Kwok, R. J. Olsson, G. Karapetrov, L. M. Paulius, W. G. Moulton, D. J. Hofman, and G. W. Crabtree, Phys. Rev. Lett. **84**, 3706 (2000).

²⁹Z. Sefrioui, D. Arias, E. M. González, C. León, J. Santamaría, and J. L. Vicent, Phys. Rev. B **63**, 064503 (2001).

³⁰J. T. Kucera, T. P. Orlando, G. Virshup, and J. N. Eckstein, Phys. Rev. B **46**, 11004 (1992).

³¹M. Tinkham, Phys. Rev. Lett. **61**, 1658 (1988).

³²Y. Yeshurun and A. P. Malozemoff, Phys. Rev. Lett. **60**, 2202 (1988).

³³R. C. Budhani, D. O. Welch, M. Suenaga, and R. L. Sabatini, Phys. Rev. Lett. **64**, 1666 (1990).

³⁴H. Yamasaki, K. Endo, S. Kosaka, M. Umeda, S. Yoshida, and K. Kajimura, Phys. Rev. B **49**, 6913 (1994).

³⁵P. Wagner, F. Hillmer, U. Frey, and H. Adrian, Phys. Rev. B **49**, 13184 (1994).

³⁶C. Attanasio, C. Coccorese, V. N. Kushnir, L. Maritato, S. L. Prischepa, and M. Salvato, Physica C **255**, 239 (1995).

³⁷M. R. Beasley, R. Labusch, and W. W. Webb, Phys. Rev. **181**, 682 (1969).

- ³⁸R. Griessen, Phys. Rev. Lett. **64**, 1674 (1990).
- ³⁹D. O. Welch, IEEE Trans. Magn. **27**, 1133 (1991).
- ⁴⁰R. Wördenweber, Rep. Prog. Phys. **62**, 187 (1999).
- ⁴¹V. Geshkenbein, A. I. Larkin, M. V. Feigel'man, and V. M. Vinokur, Physica C **162-164**, 239 (1989).
- ⁴²V. M. Vinokur, M. V. Feigel'man, V. B. Geshkenbein, and A. I. Larkin, Phys. Rev. Lett. **65**, 259 (1990).
- ⁴³W. K. Kwok, L. M. Paulius, V. M. Vinokur, A. M. Petrean, R. M. Ronningen, and G. W. Crabtree, Phys. Rev. Lett. **80**, 600 (1998).
- ⁴⁴Z. Sefrioui, D. Arias, M. Varela, J. E. Villegas, M. A. López de la Torre, C. León, G. D. Loos, and J. Santamaría, Phys. Rev. B **60**, 15423 (1999).
- ⁴⁵R. H. Koch, V. Foglietti, W. J. Gallagher, G. Koren, A. Gupta, and M. P. A. Fisher, Phys. Rev. Lett. **63**, 1511 (1989).
- ⁴⁶Y. Hidaka and M. Suzuki, Nature (London) **338**, 635 (1989).
- ⁴⁷S. H. Han, C. C. Almasan, M. C. de Andrade, Y. Dalichaouch, and M. B. Maple, Phys. Rev. B **46**, 14290 (1992).
- ⁴⁸I. W. Sumarlin, S. Skanthakumar, J. W. Lynn, J. L. Peng, Z. Y. Li, W. Jiang, and R. L. Greene, Phys. Rev. Lett. **68**, 2228 (1992).
- ⁴⁹P. Fournier and R. L. Greene, Phys. Rev. B **68**, 094507 (2003).
- ⁵⁰L. M. Paulius, J. A. Fendrich, W.-K. Kwok, A. E. Koshelev, V. M. Vinokur, G. W. Crabtree, and B. G. Glagola, Phys. Rev. B **56**, 913 (1997).
- ⁵¹D. López, L. Krusin-Elbaum, H. Safar, E. Righi, F. de la Cruz, S. Grigera, C. Feild, W. K. Kwok, L. Paulius, and G. W. Crabtree, Phys. Rev. Lett. **80**, 1070 (1998).
- ⁵²J. H. Cho, M. P. Maley, S. Fleshler, A. Lacerda, and L. N. Bulaevskii, Phys. Rev. B **50**, 6493 (1994).
- ⁵³U. Welp, W. K. Kwok, G. W. Crabtree, K. G. Vandervoort, and J. Z. Liu, Phys. Rev. Lett. **62**, 1908 (1989).